Numerical methods for coupled fracture problems

Robert C. Viesca[1], Dmitry I. Garagash[2]
Depts. [1] Civil & Env. Engng., Tufts Univ., and [2] Civil & Res. Engng., Dalhousie Univ.

30 Jul. 2017

Abstract

We consider numerical solutions in which the linear elastic response to an opening- or sliding-mode fracture couples with one or more processes. Classic examples of such problems include traction-free cracks leading to stress singularities or cracks with cohesive-zone strength requirements leading to non-singular stress distributions. These classical problems have characteristic square-root asymptotic behavior for stress, relative displacement, or their derivatives. Prior work has shown that such asymptotics lead to a natural quadrature of the singular integrals at roots of Chebyhsev polynomials of the first, second, third, or fourth kind. We show that such quadratures lead to convenient techniques for interpolation, differentiation, and integration, with the potential for spectral accuracy. We further show that these techniques, with slight amendment, may continue to be used for non-classical problems which lack the classical asymptotic behavior. We consider solutions to examples problems of both the classical and non-classical variety (e.g., fluid-driven opening-mode fracture and fault shear rupture driven by thermal weakening), with comparisons to analytical solutions or asymptotes, where available.

Keywords: fracture mechanics; cohesive zone; singular integral equations; Gauss-Chebyshev quadrature; barycentric Lagrange interpolation and differentiation; hydraulic fracture; fault rupture with thermal weakening

1 Introduction

We focus on integral equations of the (non-dimensional) form

$$\sigma(x) = \sigma_o(x) + \frac{1}{\pi}\int_{-1}^{1} K(x-s)\frac{d\delta}{ds}ds \tag{1}$$

For the crack problems we consider, x is the coordinate along which a straight crack lies. σ is the stress component whose traction is oriented either normal or parallel to the crack face and assumed to be equal in magnitude on each crack face at a given position along the crack. The relative displacement δ is the difference in displacement of each side of the crack face (i.e., crack opening or slip), with the displacement direction on each face paralleling that of the traction of σ there. A positive convention of δ is defined as that in which $\sigma\delta$ is a positive, work-conjugate product, per unit crack face area. σ_o is the traction σ that would be resolved on the crack faces in the absence of

any relative displacement. $K(\xi)$ is a kernel whose most singular term will be $1/\xi$. Equations with this form arise in, for instance, problems of in-plane, anti-plane, or axisymmetric rupture (opening or sliding) of a linear elastic material [e.g., *Hills et al.*, 1996].

Furthermore, (1) may be complemented by a system of additional equations of the form

$$G[\sigma(x), \delta(x), \xi_i(x)] = 0 \tag{2}$$

in which G is an operator that may include, but is not limited to, derivatives and convolutions involving the arguments, and $\xi_i(x)$ is a placeholder function for any number of potential fields of interest distributed, and possibly evolving, on x. These additional equations may reflect relations among the arguments determined by physical processes in addition to the elastic response to discontinuous deformation embodied in (1).

The paper is organized as follows. Section 2 presents the essentials of the numerical method, including the discrete singular (Hilbert) integral transform, interpolation, differentiation, and integration over a set of Chebyshev points. Section 3 illustrates the numerical technique on a set of crack problems of classical variety, including singular (uniform stress drop) and non-singular (cohesive) cracks. Section 4 suggests an amended numerical approach to tackle non-classical crack problems that may lack the classical square-root asymptotic behavior. This amended method is applied to the problem of an opening-mode fracture driven by the injection of a viscous fluid and the fault rupture driven by the thermal pressurization of the pore fluid in Sections 5 and 6, respectively. The final Section 7 offers a summary of main results.

2 Discretization schemes

Anticipating the range of possible systems encompassed in (1) and (2), we review numerical methods to approximately differentiate, integrate, interpolate, as well as to perform the convolution in (1). The methods are known to be spectrally accurate when the function $F(s)$ on which the operation is to be performed is analytic [e.g., *Boyd*, 2001; *Berrut and Trefethen*, 2004].

2.1 Finite Hilbert transform

We recall that Gauss-Chebyshev quadrature of a integral [e.g., *Mason and Handscomb*, 2003] takes the form

$$\int_{-1}^{1} w(s)F(s)ds \approx \sum_{j=1}^{n} w_j F(s_j) \tag{3}$$

where $w(s) = (1-s)^\alpha(1+s)^\beta$ and α and β each are $\pm 1/2$. The set of quadrature weights w_j and points s_j correspond to each possible pair of α and β (Table 1).

The above quadrature may be extended to approximate integrals with singular convolution kernels of the form

$$f(x) = \int_{-1}^{1} \frac{w(s)F(s)}{x-s} ds$$

for f evaluated at a set of points x_i (Table 1) that are complementary to the quadrature set s_j [*Erdogan et al.*, 1973]

$$f(x_i) \approx \sum_{j=1}^{n} w_j \frac{F(s_j)}{x_i - s_j}$$

Given the form of the integral equation (1), this suggests that a convenient means of evaluating the convolution integral is by the decomposition of the slip gradient

$$\frac{d\delta}{ds} = w(s)F(s)$$

where the choice of the $w(s)$ arises naturally from anticipation of the behavior of $d\delta/ds$ approaching the endpoints $s = \pm 1$, and, as will be apparent from problem examples to follow, $F(s)$ will be part of the sought solution.

Implicit in the latter quadrature is the expansion of $F(s)$ in terms of the orthogonal set of Chebyshev polynomials $\phi_k(x)$ whose weight function is $w(x)$

$$F(s) \approx \sum_{k=0}^{p} A_k \phi_k(s)$$

$\phi_k(s)$ belong to the set of Chebyshev polynomials of the first (T_k), second (U_k), third (V_k), or fourth (W_k) kind, which, with $s(\theta) = \cos\theta$), are defined by [e.g., *Mason and Handscomb*, 2003]

$$T_k[s(\theta)] = \cos(k\theta) \qquad V_k[s(\theta)] = \frac{\cos((k+1/2)\theta)}{\cos(\theta/2)}$$

$$U_k[s(\theta)] = \frac{\sin((k+1)\theta)}{\sin\theta} \qquad W_k[s(\theta)] = \frac{\sin((k+1/2)\theta)}{\sin(\theta/2)}$$

whose corresponding weight functions are in Table 1. The polynomials within a set have the orthogonality relation

$$\int_{-1}^{1} w(s)\phi_k(s)\phi_m(s)ds = \begin{cases} h(\pi) & k = m \\ 0 & k \neq m \end{cases}$$

with $h(\pi)$ given in Table 2.

If we take the coefficients A_k to be precisely defined as those which satisify

$$F(s_j) = \sum_{k=0}^{p} A_k \phi_k(s_j)$$

(requiring $p = n - 1$) we may easily retrieve the coefficients A_k of the Chebyshev polynomial expansion, if given $F(s_j)$. To do so we take advantage of discrete orthogonality relations for a set $\phi_k(s)$

$$\sum_{j=1}^{n} w_D(s_j)\phi_k(s_j)\phi_m(s_j) = \begin{cases} g(n) & k = m \\ 0 & k \neq m \end{cases}$$

(where $w_D(s_j)$ and $g(n)$ are given in Table 2), to invert for

$$A_k = \frac{1}{g(n)} \sum_{j=1}^{n} w_D(s_j)\phi_k(s_j)F(s_j)$$

or more concisely

$$A_k = \sum_{j=1}^{n} B_{kj} F(s_j)$$

where trigonometric identities permit concise expressions for B_{kj} (Table 2).

Table 1: Gauss-Chebyshev quadrature weights w_j and positions s_j, which are the roots of $\phi_n(x)$, as well as positions x_i for extension of Gauss-Chebyshev quadrature for singular convolution integrals [after *Erdogan et al.*, 1973]. $\psi_k(x)$ are the complimentary set of Chebyshev polynomials to $\phi_k(x)$. For the first row, x_i are roots of $\psi_{n-1}(x)$; for the second row, x_i are roots of ψ_{n+1}; for the remaining rows, x_i are roots of $\psi_n(x)$. For problems where the interval $x \in (0, \infty)$ is mapped to $z \in (-1, 1)$, z and u take the place of x and s.

$\phi_k(s)$	$w(s)$	w_j/π	s_j	x_i	i	$\psi_k(x)$
$T_k(s)$	$\frac{1}{\sqrt{1-s^2}}$	$\frac{1}{n}$	$\cos\left(\frac{\pi(j-1/2)}{n}\right)$	$\cos\left(\frac{\pi i}{n}\right)$	$i = 1, ..., n-1$	$U_k(x)$
$U_k(s)$	$\sqrt{1-s^2}$	$\frac{1-s_j^2}{n+1}$	$\cos\left(\frac{\pi j}{n+1}\right)$	$\cos\left(\frac{\pi(i-1/2)}{n+1}\right)$	$i = 1, ..., n+1$	$T_k(x)$
$V_k(s)$	$\sqrt{\frac{1+s}{1-s}}$	$\frac{1-s_j}{n+1/2}$	$\cos\left(\frac{\pi(j-1/2)}{n+1/2}\right)$	$\cos\left(\frac{\pi i}{n+1/2}\right)$	$i = 1, ..., n$	$W_k(x)$
$W_k(s)$	$\sqrt{\frac{1-s}{1+s}}$	$\frac{1+s_j}{n+1/2}$	$\cos\left(\frac{\pi j}{n+1/2}\right)$	$\cos\left(\frac{\pi(i-1/2)}{n+1/2}\right)$	$i = 1, ..., n$	$V_k(x)$

2.2 Interpolation

Given $F(s_j)$, we may use the above truncated Chebyshev polynomial expansion to provide an interpolation for $F(x_i)$ as

$$F(x_i) \approx \sum_{k=0}^{n-1} A_k \phi_k(x_i)$$

recalling that the coefficients A_k are determined by $F(s_j)$,

$$F(x_i) \approx \sum_{k=0}^{n-1} \sum_{j=1}^{n} B_{kj} F(s_j) \phi_k(x_i)$$

which may be more simply written in terms of an interpolation matrix L_{ij}

$$F(x_i) \approx \sum_{j=1}^{n} L_{ij} F(s_j)$$

where

$$L_{ij} = \sum_{k=0}^{n-1} \phi_k(x_i) B_{kj}$$

The function $F(s)$ was carried forward from the previous section as a convenient, nominal example, and we emphasize that this interpolation method may be used to interpolate any function whose values at points s_j are known or presumed. Likewise, the interpolation may be done to any set of points x_i (i.e., not just the set of points complementary to s_j defined in Table 1).

We note that due to uniqueness of the interpolating polynomial of order $n-1$ fitting a function at n points [e.g., *Powell*, 1981], L_{ij} will be identical to an interpolation matrix derived from

Table 2: Discrete orthogonality weights $w_D(s_j)$, discrete inner product values $g(n)$, continuous inner product values $h(\pi)$, and matrix B_{kj} for inferring Chebyshev polynomial expansion coefficients A_k given known collocation point values $F(s_j)$. We use the shorthand $\theta_j = \arccos(s_j)$.

$\phi_k(s)$	$w_D(s_j)$	$g(n)$	$h(\pi)$	B_{kj}
$T_k(s)$	1	$\begin{cases} n & k=0 \\ n/2 & k>0 \end{cases}$	$\begin{cases} \pi & k=0 \\ \pi/2 & k>0 \end{cases}$	$\begin{cases} 1/n & k=0 \\ 2\cos(k\theta_j)/n & k>0 \end{cases}$
$U_k(s)$	$1-s_j^2$	$\dfrac{n+1}{2}$	$\pi/2$	$\dfrac{2\sin(\theta_j)\sin((k+1)\theta_j)}{n+1}$
$V_k(s)$	$1+s_j$	$n+\dfrac{1}{2}$	π	$\dfrac{2\cos(\theta_j/2)\cos((k+1/2)\theta_j)}{n+1/2}$
$W_k(s)$	$1-s_j$	$n+\dfrac{1}{2}$	π	$\dfrac{2\sin(\theta_j/2)\sin((k+1/2)\theta_j)}{n+1/2}$

other means of constructing the polynomial interpolant from the set of points s_j. The celebrated barycentric form of Lagrange interpolation [e.g., *Berrut and Trefethen*, 2004] is a very convenient alternative and represents L_{ij} as

$$L_{ij} = \left(\frac{\omega_j}{x_i - s_j}\right) \Big/ \left(\sum_{m=1}^{n} \frac{\omega_m}{x_i - s_m}\right) \tag{4}$$

where the weights ω_j depend on the set of points s_j and are provided in Table 3.

This latter expression for L_{ij} has several advantages over the former. The foremost is that switching among the set of points s_j simply requires an accompanying switch in the weights ω_j: no other explicit consideration of the Chebyshev polynomial kind is needed to evaluate the entries of L_{ij}. Additionally, the latter expression (4) carries the same advantage for constructing a differentiation matrix, as will be noted in the following section. Another, comparatively minor advantage is that the barycentric form, along with trigonometric identities, quickly leads to simple expressions for interpolating to the endpoints ± 1

$$F(-1) \approx \sum_{j=1}^{n} P_j F(s_j), \qquad F(1) \approx \sum_{j=1}^{n} Q_j F(s_j)$$

where the vectors P_j and Q_j for each set of s_j are provided in Table 3. The expressions for P_j and Q_j therein provide concise alternatives to those given by *Krenk* [1975b].

2.3 Differentiation

The truncated Chebyshev expansion of a function permits a straightforward estimation of the derivative, e.g., at points s_j. Here, for example, the expansion of $F(s)$ leads to

$$F'(s_j) \approx \sum_{k=0}^{p} A_k \phi_k'(s_j)$$

Table 3: Weights ω_j for the barycentric form of Lagrange polynomial interpolation using $F(s_j)$; weights ω_i for interpolation using $F(x_i)$; vectors P_j and Q_j to interpolate using $F(s_j)$ to find $F(\pm 1)$, respectively. We continue to use the shorthand $\theta_j = \arccos(s_j)$ and introduce $\theta_i = \arccos(x_i)$, where s_j and x_i are those sets of points which correspond to a given set of polynomials ϕ_k from Table 1.

$\phi_k(s)$	$\omega_j/(-1)^j$	$\omega_i/(-1)^i$	$P_j/(-1)^j$	$-Q_j/(-1)^j$
$T_k(s)$	$\sin(\theta_j)$	$\sin^2(\theta_i)$	$\dfrac{\tan(\theta_j/2)}{n}$	$\dfrac{\cot(\theta_j/2)}{n}$
$U_k(s)$	$\sin^2(\theta_j)$	$\sin(\theta_i)$	$\sin^2(\theta_j/2)$	$2\cos^2(\theta_j/2)$
$V_k(s)$	$\cos(\theta_j/2)\sin(\theta_j)$	$\sin(\theta_i/2)\sin(\theta_i)$	$2\sin(\theta_j/2)$	$\dfrac{\cos(\theta_j/2)\cot(\theta_j/2)}{n+1/2}$
$W_k(s)$	$\sin(\theta_j/2)\sin(\theta_j)$	$\cos(\theta_i/2)\sin(\theta_i)$	$-\dfrac{\sin(\theta_j/2)\tan(\theta_j/2)}{n+1/2}$	$2\cos(\theta_j/2)$

However, expressions for $\phi_k'(s)$ are only concisely written for the case of the Chebyshev polynomial of the first kind: $T_k'(x) = kU_{k-1}(x)$. For the remaining kinds, expressions of the derivatives in terms of Chebyshev polynomials are comparatively cumbersome. Nevertheless, recalling that A_k are defined in terms of $F(s_j)$, we may construct a differentiation matrix $D_{jj'}$

$$F'(s_j) \approx \sum_{k=0}^{n-1} A_k \phi_k'(s_j) = \sum_{k=0}^{n-1} \sum_{j'=1}^{n} B_{kj'} F(s_{j'}) \phi_k'(s_j) = \sum_{j'=1}^{n} D_{jj'} F(s_{j'})$$

where here

$$D_{jj'} = \sum_{k=0}^{n-1} B_{kj'} \phi_k'(s_j)$$

However, again owing to the uniqueness of the polynomial interpolant, the barycentric form of the Lagrange polynomial interpolation provides an identical differentiation matrix that is more conveniently expressed for all sets of points s_j as [*Berrut and Trefethen*, 2004]

$$D_{jj'} = \frac{\omega_{j'}/\omega_j}{s_j - s_{j'}} \qquad j \neq j' \tag{5a}$$

$$D_{jj} = -\sum_{j'=1, j' \neq j}^{n} D_{jj'} \tag{5b}$$

where here the weights ω_j are those found in Table 3.

2.4 Integration

We now look for techniques to evaluate integrals such as

$$\delta(x) - \delta(-1) = \int_{-1}^{x} \frac{d\delta}{ds} ds = \int_{-1}^{x} w(s) F(s) ds$$

Table 4: Function $\Phi_k(x)$ for use in developing an integral quadrature.

$\phi_k(s)$	$-\Phi_0(x)$	$-\Phi_k(x), k>0$
$T_k(s)$	θ	$\dfrac{\sin(k\theta)}{k}$
$U_k(s)$	$\dfrac{1}{2}\left(\theta - \dfrac{\sin(2\theta)}{2}\right)$	$\dfrac{1}{2}\left(\dfrac{\sin(k\theta)}{k} - \dfrac{\sin((k+2)\theta)}{k+2}\right)$
$V_k(s)$	$\theta + \sin\theta$	$\dfrac{\sin(k\theta)}{k} + \dfrac{\sin((k+1)\theta)}{k+1}$
$W_k(s)$	$\theta - \sin\theta$	$\dfrac{\sin(k\theta)}{k} - \dfrac{\sin((k+1)\theta)}{k+1}$

To do so, we use the result that

$$\int_{-1}^{x} w(s)\phi_k(s)ds = \Phi_k(x) - \Phi_k(-1)$$

(where the corresponding $\Phi_k(x)$ are given in Table 4) such that the approximation of $F(s)$ in terms of a truncated Chebyshev polynomial expansion in $\phi_k(s)$ leads to

$$\delta(x) - \delta(-1) \approx \sum_{k=0}^{n-1} A_k[\Phi_k(x) - \Phi_k(-1)]$$

Recalling that A_k are determined by $F(s_j)$ via B_{kj}, we may write the above approximation as

$$\delta(x) - \delta(-1) \approx \sum_{k=0}^{n-1}\sum_{j=1}^{n} B_{kj}F(s_j)[\Phi_k(x) - \Phi_k(-1)]$$

If we restrict ourselves to a set of points x_i, the approximation is

$$\delta(x_i) - \delta(-1) \approx \sum_{j=1}^{n} S_{ij}F(s_j)$$

where

$$S_{ij} = \sum_{k=0}^{n-1}[\Phi_k(x_i) - \Phi_k(-1)]B_{kj}$$

3 Classical fracture examples

Here we highlight numerical solutions using the above discretization schemes to problems with known or previously unknown solutions. The problems are of the classical variety, which we define as a problem in which, aside from so-called cohesive zone laws, there are no additional equations of the form of $G = 0$ to be satisfied, and that the end-point asymptotic behavior is of the square-root variety of the Chebyshev polynomial weight functions.

3.1 Crack with uniform stress drop (single solution)

We begin by considering the classical problem of a traction-free crack of length $2a$ under a uniform far-field loading σ_o. The dimensional form of the problem is

$$\sigma(x) = \sigma_o - \frac{\mu'}{2\pi}\int_{-a}^{a}\frac{d\delta/ds}{x-s}ds \tag{6}$$

where $\sigma(x) = 0$ for $|x| < a$ and the modulus $\mu' = \mu/(1-\nu)$ for modes I and II (plane strain), and $\mu' = \mu$ for mode III, with μ being the shear modulus and ν the Poisson ratio of the medium hosting the crack. After non-dimensionalization $x/a \Rightarrow x$ and $\delta\mu'/(2\sigma_o a) \Rightarrow \delta$, the problem becomes

$$1 = \frac{1}{\pi}\int_{-1}^{1}\frac{d\delta/ds}{x-s}ds \quad \text{for } |x| < 1$$

Anticipating, due to the crack singularity, that $d\delta/ds \sim 1/\sqrt{1-|s|}$ as $|s| \to 1$, we look for a solution of the form $d\delta/ds = F(s)/\sqrt{1-s^2}$, the Gaussian quadrature for the singular integral implies the discretization

$$1 \approx \frac{1}{\pi}\sum_{j=1}^{n} w_j \frac{F(s_j)}{x_i - s_j} \tag{7}$$

with, as can be read in Table 1,

$$s_j = \cos\left(\pi\frac{2j-1}{2n}\right),\ j = 1, ..., n$$

$$x_i = \cos\left(\pi\frac{i}{n}\right),\ i = 1, ..., n-1$$

$$w_j = \frac{\pi}{n}$$

The discretization yields n-unknowns $F(s_j)$ and only $n-1$ equations. This under-determinancy is resolved by an additional constraint. Such a constraint is the anticipated symmetry of the relative displacement δ or zero cumulative relative displacement, respectively,

$$\frac{d\delta(s=0)}{ds} = 0 \to \phi(0) = 0,$$
$$0 = \delta(1) - \delta(-1) = \int_{-1}^{1}\frac{d\delta}{ds}ds = \int_{-1}^{1}\frac{F(s)}{\sqrt{1-s^2}}ds \approx \sum_{j=1}^{n} w_j F(s_j)$$

Solving the system of equations (7) with either of the last two constraints provides the approximate solution. The known solution is $\delta(x) = \sqrt{1-x^2}$, for which $F(s) = -s = -T_1(s)$. Given the basis for our discretization, the approximate solution for $\delta(x)$ is expected and observed to be computed to within machine precision of the known solution for $n \geq 2$.

3.2 Cohesive-zone crack (one-parameter family of solutions)

A variation of the above problem that results in a one-parameter family of solutions is to impose a simple strength criterion on the crack interface. Specifically, we imagine the Dugdale-Barenblatt scenario of a crack, again under uniform far-field loading σ_o, whose interface has a peak strength σ_p up to a critical relative displacement δ_c, beyond which the strength reduces to a residual value σ_r (which may be zero). This problem is given by (6) where now

$$\sigma(x) = \begin{cases} \sigma_p & 0 < \delta(x) < \delta_c \\ (\sigma_p + \sigma_r)/2 & \delta(x) = \delta_c \\ \sigma_r & \delta(x) > \delta_c \end{cases} \tag{8}$$

for $|x| < a$. If the relative displacement increases monotonically from the end-points of the crack towards the interior, we may impose the strength condition in terms of a known spatial distribution of stress, where $x = \pm c$ is the position at which the relative displacement reaches the critical value. The problem is then alternatively posed as

$$\sigma_o - \frac{\mu'}{2\pi}\int_{-a}^{a} \frac{d\delta/ds}{x-s} ds = \begin{cases} \sigma_p & c < |x| < a \\ (\sigma_p + \sigma_r)/2 & |x| = c \\ \sigma_r & |x| < c \end{cases}$$

With $x/a \Rightarrow x$, $\delta\mu'/[2(\sigma_p - \sigma_r)a] \Rightarrow \delta$, $c/a \Rightarrow c$ and $(\sigma_o - \sigma_r)/(\sigma_p - \sigma_r) \Rightarrow r$, this latter problem non-dimensionalizes to

$$r - \frac{1}{\pi}\int_{-1}^{1} \frac{d\delta/ds}{x-s} ds = \begin{cases} 1 & c < |x| < 1 \\ 1/2 & |x| = c \\ 0 & |x| < c \end{cases} \qquad \text{where } 0 < r, c < 1 \tag{9}$$

Requiring a non-singular stress distribution at the crack tips implies $d\delta/ds \sim \sqrt{1-|s|}$ as $|s| \to 1$. Therefore, we look for solutions of the form $d\delta/ds = \sqrt{1-s^2}F(s)$, and the problem discretizes to

$$r - \frac{1}{\pi}\sum_{j=1}^{n} w_j \frac{F(s_j)}{x_i - s_j} = \begin{cases} 1 & c < |x_i| < 1 \\ 1/2 & |x_i| = c \\ 0 & |x_i| < c \end{cases} \tag{10}$$

where s_j, x_i, and w_j are those found in Table 1 corresponding to $w(s) = \sqrt{1-s^2}$. Here we have n unknowns $F(s_j)$, and $n+1$ equations. For a given r, we have the additional unknown $c(r)$. The solution for the crack half length a can be recovered from the value of the normalized displacement discontinuity at the cohezive zone edge, $\delta(c)$ which, as per the scaling used, is equal to the normalized critical displacement $\delta_c\mu'/[2(\sigma_p - \sigma_r)a]$. Alternatively, we may consider that c is specified and the unknown is $r(c)$. Practically speaking, the latter approach provides more accurate solutions and is also more readily implementable for the problem as posed in (10) given than we may assign the positions $\pm c$ to gridpoints of x_i.

For comparison, we present the closed-form solution to the problem of an in-plane or anti-plane Dugdale-Barenblatt cohesive zone crack. To begin we note that the absence of a stress singularity

of the crack tips, requires that the stress distribution of the dimensional problem satisfies [e.g., *Rice*, 1968]

$$\int_{-a}^{a} \frac{\sigma(x) - \sigma_o}{\sqrt{a^2 - x^2}} dx = 0 \tag{11}$$

which implies, after non-dimensionalizing as for (9), that $c = \sin[(1-r)\pi/2]$. Continuing to follow the scaling as in (9), we note that after taking the derivative of (9) and integrating the integral transform by parts, we arrive to

$$-\frac{1}{\pi} \int_{-1}^{1} \frac{d^2\delta/ds^2}{x-s} ds = \frac{d\sigma}{dx}, \quad \frac{d\sigma}{dx} = -\delta_D(x+c) + \delta_D(x-c)$$

(where $\delta_D(x)$ is the Dirac delta function). This integral equation may be inverted [e.g., *Mushkelishvili*, 1953] to

$$\frac{d^2\delta}{dx^2} = \frac{C}{\sqrt{1-x^2}} + \frac{1}{\sqrt{1-x^2}} \frac{1}{\pi} \int_{-1}^{1} \frac{\sqrt{1-s^2}}{x-s} \frac{d\sigma}{ds} ds$$

where the constant C is determined by requiring that $\int_{-1}^{1} (d^2\delta/dx^2) dx = 0$. The relative displacement δ and its gradient is determined by also requiring that $\delta(\pm 1) = 0$ and $\delta'(\pm 1) = 0$. Imposing these conditions we find that $C = 0$,

$$\frac{d^2\delta}{dx^2} = \frac{1}{\pi} \sqrt{\frac{1-c^2}{1-x^2}} \frac{c}{x^2-c^2}, \quad \frac{d\delta}{dx} = \frac{1}{2\pi c\sqrt{1-c^2}} \ln \left| \frac{x\sqrt{1-c^2} - c\sqrt{1-x^2}}{x\sqrt{1-c^2} + c\sqrt{1-x^2}} \right|$$

and

$$\delta(x) = \frac{c}{\pi} \ln \left| \frac{c^2 - x^2}{(\sqrt{1-c^2} - \sqrt{1-x^2})^2} \right| + \frac{x}{\pi} \ln \left| \frac{x\sqrt{1-c^2} - c\sqrt{1-x^2}}{x\sqrt{1-c^2} + c\sqrt{1-x^2}} \right|$$

The solution to this classic problem was first found by other means with alternative scalings by *Bilby et al.* [1963].

In Figure 1 we compare the results from the approximate solution given by the solution to the discretized system of equations to the above exact solution. We find that the method is second-order accurate with n in solving for the slip distribution $\delta(x)$. We find that the solution for r is computed to machine precision for all n.

As a brief aside, we consider an alternative to the numerical solution procedure proposed to arrive at the system (10). Specifically, we consider a search for a solution by choosing a value of r and letting c be determined as part of the problem solution. To do so, we must consider the problem as posed in (13). However, for an arbitrarily chosen value of $0 < r < 1$, the point c is imprecisely determined as it likely will fall between collocation points. Numerical solutions found by this route are less accurate than those found when seeking $r(c)$. Proceeding nevertheless, we may nondimensionalize (13) with $\delta/\delta_c \Rightarrow \delta$, $x/a \Rightarrow x$, and $2a(\tau_p - \tau_r)/(\mu'\delta_c) \Rightarrow a$ to arrive to

$$r - \frac{1}{\pi a} \int_{-1}^{1} \frac{d\delta/ds}{x-s} ds = \begin{cases} 1 & 0 < \delta(x) < 1 \\ 1/2 & \delta(x) = 1 \\ 0 & \delta(x) > 1 \end{cases}$$

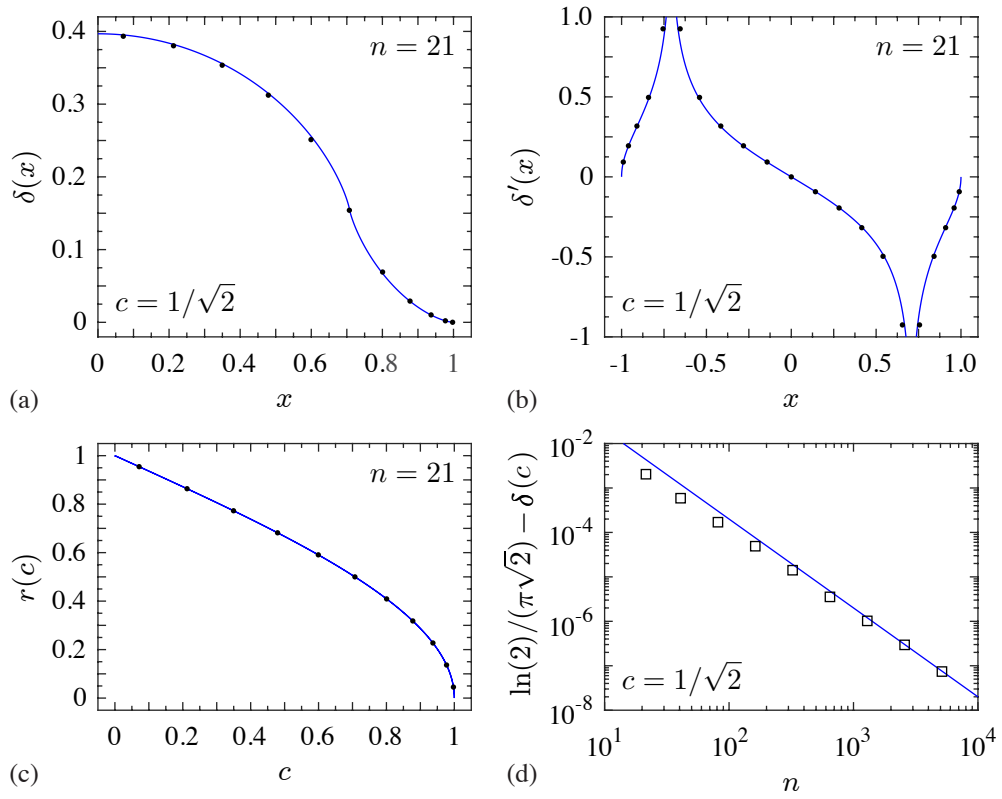

Figure 1: For the problem of a Dugdale-Barenblatt cohesive zone crack in equilibrium with a uniform far-field loading, in (a–c) we compare the exact solution (curves) to the approximate solution (dots) with a fixed value of n (the number of points s_j), and in (d) we show how a residual vanishes with increasing n to show the rate of convergence. (a) and (b) show the distribution of the relative displacement (symmetric about $x = 0$) and its derivative for a fixed value of the problem parameter c. Note the singularity in the latter at $x = \pm c$. (c) shows how one variable of the problem solution, the scaled background loading stress r, varies with the parameter c, which is the position at which the strength drops from a peak to a residual value. As part of the solution, the position c is chosen to coincide with a point in the set x_i. (d) The difference between the true solution and the approximate solution for the relative displacement at a fixed position ($x = c$) decreases with an increasing n in a manner indicating that the method is second-order accurate in n (line here is $2/n^2$).

With this scaling, we see that if we fix the parameter r, the nondimensional crack length a is now the additional unknown. The discretized problem is

$$r - \frac{1}{\pi a}\sum_{j=1}^{n} w_j \frac{F(s_j)}{x_i - s_j} = \begin{cases} 1 & \delta(x_i) > 1 \\ 1/2 & \delta(x_i) = 1 \\ 0 & \delta(x_i) < 1 \end{cases} \quad \text{with } \delta(x_i) = \sum_{j=1}^{n} S_{ij} F(s_j) \tag{12}$$

where w_j, x_i, and s_j are as before, and S_{ij} is the integration quadrature matrix.

An adjustment to this alternative approach that would preserve solution accuracy would be to add the constraint that at the m-th gridpoint, $\delta(x_m) = 1$ (where $1 \leq m \leq n$), allowing for both r and a to be considered as unknowns in addition to $F(s_j)$, and, with the scaling $c/a \Rightarrow c$, identifying $\pm x_m$ as $\pm c$. The slip at x_m may be approximated as

$$\delta(x_m) = \int_{-1}^{x_m} \frac{d\delta}{ds} ds \approx \sum_{j=1}^{n} S_{mj} F(s_j)$$

where the quadrature vector S_{mj} is pulled from a row of the quadrature matrix S_{ij}. This additional equation completes the system to allow for the solution of $F(s_j)$, c, and a.

Here we take the opportunity to make a brief aside on the accuracy of this approach for cohesive zone problems. We note that the solution for $\delta(x)$ contains logarithmic singularities in $\delta'(x)$, and thus in $F(s)$ as well, at $s = \pm c$. Consequently, the numerical solution is only second-order accurate. This logarithmic singularity is owed to the discontinuity in the Dugdale-Barenblatt cohesive zone relation $\sigma(\delta)$. Generally, a discontinuity in the m-th derivative of a cohesive zone relation gives rise to a logarithmic singularity in the m-th derivative of $F(s)$ (or stated alternatively, a discontinuity in $d^m\sigma/dx^m$ within an interior point ($|s| < 1$) gives rise to a logarithmic singularity in $d^{(m+1)}\delta/dx^{(m+1)}$ at that point; Appendix A). However, while eliminating discontinuities in the cohesive zone law or its derivatives, i.e., when $\sigma(\delta)$ is an analytic function, is sufficient to ensure there are no singularities present in $F(s)$ or its derivatives for $|s| < 1$, any cohesive zone law that linearizes about $\delta = 0$ will yield a logarithmic singularity in $F'(\pm 1)$ (Appendix A). However, we also show in Appendix A that the absence of such a linearization (i.e., when $d\sigma/d\delta = 0$ at $\delta = 0$) eliminates that end-point singularity. As a result, if the cohesive relation is, for instance, an exponential weakening $\sigma(\delta) = \sigma_p - (\sigma_p - \sigma_r)\exp(-\delta/\delta_c)$, which linearizes about $\delta = 0$, the end-point singularity is present and we expect the method to be fourth-order accurate in n. However, the minor modification to a half-bell-curve distribution of cohesive strength with slip $\sigma(\delta) = \sigma_p - (\sigma_p - \sigma_r)\exp[-(\delta/\delta_c)^2]$ eliminates the singularity in F', as well as higher-order derivatives, such that $F(s)$ is now analytic, leading to the expectation of spectral convergence. These expectations are confirmed in practice (Figure 2), where for exponential slip-weakening, the problem is

$$\sigma_o - \frac{\mu'}{2\pi}\int_{-a}^{a} \frac{d\delta/ds}{x - s} ds = \sigma_p - (\sigma_p - \sigma_r)\exp(-\delta/\delta_c) \tag{13}$$

With $x/a \Rightarrow x$, $\delta/\delta_c \to \delta$, $2a(\sigma_p - \sigma_r)/(\mu'\delta_c) \Rightarrow a$, and $(\sigma_o - \sigma_r)/(\sigma_p - \sigma_r) \Rightarrow r$, this problem non-dimensionalizes to

$$r - \frac{1}{\pi a}\int_{-1}^{1} \frac{d\delta/ds}{x - s} ds = \exp(-\delta) \tag{14}$$

where, for a given r, the solution consists of $\delta(x)$ and a. The quadratic-exponential weakening is treated similarly and the discretization of both is as for the Dugdale-Barenblatt problem as posed in (12).

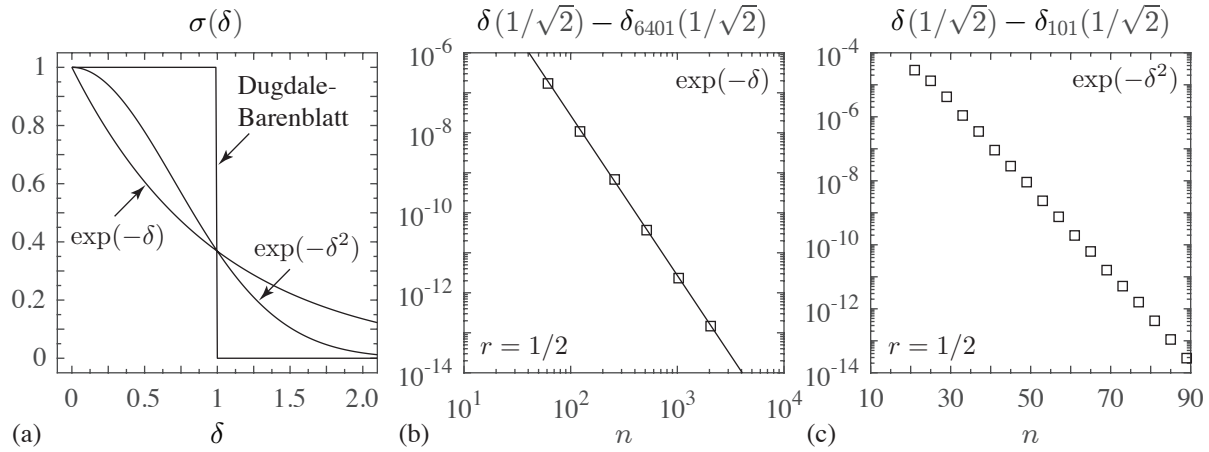

Figure 2: (a) Illustration of Dugdale-Barenblatt, exponential weakening, and quadratic-exponential weakening cohesive zone relations. Considering the problem of a cohesive-zone crack in equilibrum with a uniform background stress ($r = 1/2$), we demonstrate the improvement from (b) fourth-order to (c) exponential convergence with n by a change of the cohesive zone law from one that linearizes about $\delta = 0$ (exponential) to one whose leading-order term is quadratic (quadratic-exponential). Given that analytical solutions for the problems of (b–c) do not exist, convergence is determined by observing the decay of residuals calculated by substracting from solutions at each n a solution for which (b) $n = 6401$ and (c) $n = 101$.

As a minor aside, we note that for cohesive cracks in which we write $\sigma(\delta)$, such as the two exponential forms above or the piecewise linear form considered in the next section (and not alternatively written as $\sigma(x)$, as in the Dugdale-Barenblatt problem), it may be shown that solutions are not unique. Rather, for a given value of r, there may exist a countably infinite family of solutions [e.g., *Dempsey et al.*, 2010], only a subset of which may be symmetric and also respect physical principles underlying the cohesive law (e.g., that of frictional resistance for sliding-mode cracks). In Figure 2, the solutions are those for which δ is symmetric and monotonically increasing from the crack tips $x = \pm 1$ toward the center $x = 0$. An alternative pulse-like solution, characterized by a monotonic accumulation of the displacement discontinuity along the crack, has been explored by Garagash [2012] in the case of the exponential cohesive law. Other cohesive-zone problems in which the procedure used here has been applied and documented in detail include *Viesca and Rice* [2012] and *Brantut and Viesca* [2015].

3.3 Cohesive zone tip solution (single solution with semi-infinite domain)

Here we consider a semi-infinite crack in equilibrium with a background load σ_o, and whose strength weakens linearly with relative displacement from a peak value, σ_p to a residual, σ_r, over a critical amount of displacement δ_c, [*Ida*, 1972] or

$$\sigma_o - \frac{\mu'}{2\pi}\int_0^\infty \frac{d\delta/ds}{x-s} = \begin{cases} \sigma_p - (\sigma_p - \sigma_r)\dfrac{\delta(x)}{\delta_c} & 0 < \delta(x) \le \delta_c \\ \sigma_r & \delta(x) \ge \delta_c \end{cases} \tag{15}$$

For this problem, due to equilibrium considerations, we require that the background loading $\sigma_o = \sigma_r$, the residual strength. We define the distance R as that at which the relative displacement reaches the critical value, $\delta(R) = \delta_c$. Choosing the scalings $x/R \Rightarrow x$, $\delta/\delta_c \Rightarrow \delta$, and $2R(\sigma_p - \sigma_r)/(\mu'\delta_c) \Rightarrow R$, the problem non-dimensionalizes to

$$\frac{1}{\pi R}\int_0^\infty \frac{d\delta/ds}{s-x}ds = \begin{cases} 1-\delta(x) & 0 < \delta(x) \le 1 \\ 0 & \delta(x) \ge 1 \end{cases}$$

In analogy to the last formulation of the cohesive zone crack problem in the previous section (in which we needed to determine δ, a, and r), here the problem is that of determining the slip δ and the distance R. However, the problem is posed on a semi-infinite interval; nonetheless, we may pursue a solution by using an appropriate change of variable to transform the problem to one on a finite domain, in which we may use the convenient Gaussian quadrature for the finite Hilbert transform.

We use the following coordinate transformation from $x \in (0, \infty)$ to $z \in (-1, 1)$

$$x(z) = \frac{1+z}{1-z}, \; \frac{dx}{dz} = \frac{2}{(1-z)^2}$$

to transform (15) into a problem of the form,

$$\frac{1}{\pi R}\int_{-1}^{1} \frac{g(u)}{u-z}du = h(z) \tag{16}$$

where

$$g(u) = (1-u)\frac{d\delta[s(u)]}{du}$$
$$h(z) = \begin{cases} 2(1-\delta[x(z)])/(1-z) & 0 < \delta[x(z)] \le 1 \\ 0 & \delta[x(z)] \ge 1 \end{cases}$$

To evaluate the left hand side of (16) using the Gaussian quadrature, we look to find an appropriate weight function for the decomposition of g. The non-singular stress condition at the crack tip and the uniform stress drop imply the following asymptotic scalings for $d\delta/ds$

$$\left.\frac{d\delta}{ds}\right|_{s\to 0} \sim \sqrt{s} \qquad \left.\frac{d\delta}{ds}\right|_{s\to\infty} \sim \frac{1}{\sqrt{s}}$$

which imply that, at its endpoints, $g(u)$ behaves as

$$g(u \to -1) \sim \sqrt{1+u}, \qquad g(u \to 1) \sim \frac{1}{\sqrt{1-u}}$$

suggesting the appropriate decomposition is

$$g(u) = \sqrt{\frac{1+u}{1-u}}F(u)$$

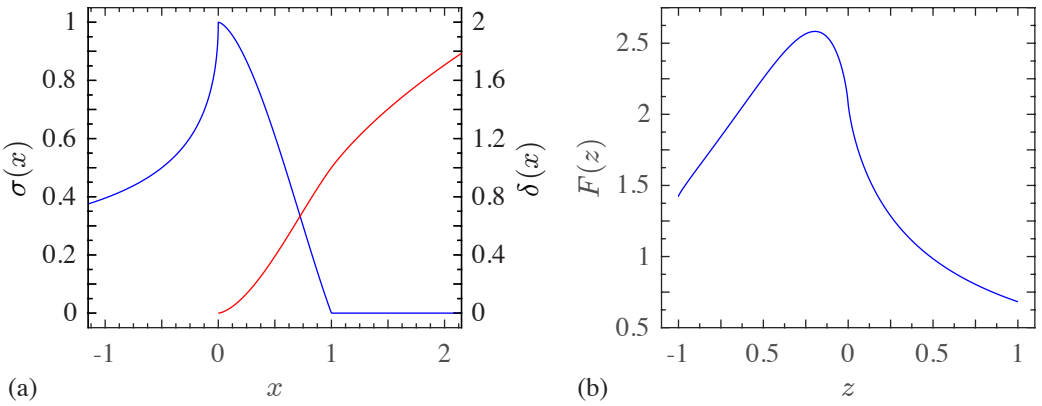

Figure 3: (a) Distributions of stress (blue) and relative displacement (red) with distance x behind the crack tip of a fracture whose strength weakens relative displacement in a piecewise-linear fashion, as found by numerical solution. (b) Distribution of the solution variable $F(z)$, where $d\delta/dx = F[z(x)]\sqrt{x/(1+x)^2}$ and $z(x) = (x-1)/(x+1)$ is the compactly mapped spatial coordinate. Analytical expressions for limit values $F(\pm 1)$ are given in the main text for validation.

problem discretizes to

$$\frac{1}{\pi R}\sum_{j=1}^{n} w_j \frac{F(u_j)}{u_j - z_i} = \begin{cases} 2(1-\delta[x(z_i)])/(1-z_i) & 0 < \delta[x(z_i)] \leq 1 \\ 0 & \delta[x(z_i)] \geq 1 \end{cases} \tag{17}$$

where u_j, z_i, and ω_j are those found in Table 1 corresponding to $w(u) = \sqrt{(1+u)/(1-u)}$. The above provides only n equations for $n+1$ unknowns $F(u_j)$ and R.

The necessary additional constraint comes from requiring that $\delta(1) = 1$. The position $x = 1$ corresponds to $z = 0$, which does not exist within the sets of quadrature points u_j and z_i for this problem. Instead, to impose this constraint, we first calculate

$$\delta[x(z_i)] - \delta[x(-1)] = \int_{-1}^{z_i} \frac{d\delta}{du} du = \int_{-1}^{z_i} \frac{g(u)}{1-u} du = \int_{-1}^{z_i} \sqrt{\frac{1+u}{1-u}} \frac{F(u)}{1-u} du \approx \sum_{j=1}^{n} S_{ij} \frac{F(u_j)}{1-u_j}$$

where the matrix S_{ij} is determined by the integration scheme from the previous section corresponding to $w(u) = \sqrt{(1+u)/(1-u)}$. The crack tip relative displacement $\delta[x(-1)] = 0$. Using the resulting expression for $\delta[x(z_i)]$ we may then interpolate to find

$$\delta[x(0)] \approx \sum_{i=1}^{n} M_i \delta[x(z_i)]$$

where the interpolation vector M_i constructed by substituting 0 for x_i and z_i, z_m for s_j, s_m in (4) and using the weights $\omega_i = (-1)^i \sin(\theta_i/2)\sin(\theta_i)$ from Table 4 with $\theta_i = \arccos(z_i)$. Requiring this approximate value of $\delta(1)$ to equal 1 provides the additional constraint.

In Figure 3 we show the solution to the discretized problem, in which $R = 1.46229...$. Figure 3a shows the distribution of stress and relative displacement with distance behind the crack tip x. Stress ahead of the crack tip ($x < 0$) is calculated at the set of points $x_i = (z_i - 1)/(z_i + 1)$. We

compute $\sigma(x_i)$ by evaluating the left hand side of (17) with $z_i^{out} = z(x_i) = -1/z_i$ in place of z_i, u_j as defined previously, and R and $F(u_j)$ from the solution. The points z^{out} lie outside the interval $(-1, 1)$. While this problem eludes an exact solution, as a convenient validation, we show in what follows that we may anticipate the value of $F(1)$ and have a consistency check for the value $F(-1)$.

The value of $F(1)$ reflects the asymptotic behavior of the slip gradient as $x \to \infty$, which is determined by using a small-scale yielding analysis [e.g., *Rice*, 1968]. A stress intensity factor for a tip of a crack dictates the strength of the stress singularity just ahead of a singular crack tip is of the form $\sigma(x) = K/\sqrt{2\pi(-x)}$, where $-x$ is the distance ahead of the tip, as taken in (15). Such singular cracks have relative displacements of $\delta(x) = 2(K/\mu')\sqrt{2x/\pi}$ when approaching the crack tip. The energy release rate of such singular cracks is given by $K^2/(2\mu')$. When considering non-singular cohesive zone cracks with a proscribed cohesive law $\sigma(\delta)$, the fracture energy $G = \int_0^{\delta_c}[\sigma(\delta) - \sigma_r]d\delta$ [e.g., *Palmer and Rice*, 1973], which is $G = (\sigma_p - \sigma_r)\delta_c/2$ for the piecewise-linear weakening relation of this section. The small-scale-yielding approximation of a cohesive-zone crack is its representation as a singular crack for $x \gg R$ with an effective stress intensity factor K determined by matching the energy release rate for the singular crack with the fracture energy G. For the cohesive law of this section this implies $K = \sqrt{\mu'(\sigma_p - \sigma_r)\delta_c}$. Switching to dimensionless variables by taking the scalings of this section results in the asymptotic behavior of the relative displacement as $x \to \infty$ taking the form

$$\frac{d\delta}{dx} = \sqrt{\frac{2(\sigma_p - \sigma_r)\delta_c/\mu'}{\pi x}} \quad \Rightarrow \quad \frac{d\delta}{dx} = \sqrt{\frac{R}{\pi x}}$$

With the change of coordinates from x to z and the decomposition $(1 - z)d\delta/dz = w(z)F(z)$, this asymptotic behavior requires that

$$F(1) = \sqrt{\frac{R}{\pi}} \approx 0.6822...$$

On the other hand, the value of $F(-1)$ reflects the asymptotic behavior of approaching the crack tip, or $x \to 0$, the determination of which requires explicit consideration of evolution within the cohesive zone, the details of which were previously subsumed in the small-scale-yielding approximation. We begin by considering the scaled version of (15), taking a spatial derivative, and integrating by parts to arrive to

$$-\frac{1}{\pi R}\int_0^\infty \frac{d^2\delta/ds^2}{s - x} = \frac{d\sigma}{dx}$$

This equation may be inverted [e.g., *Rice*, 1968]

$$\frac{d^2\delta}{dx^2} = \frac{C}{\sqrt{x}} + \frac{R}{\pi\sqrt{x}}\int_0^\infty \frac{\sqrt{s}}{x - s}\frac{d\sigma}{ds}ds$$

where C is a constant determined by requiring that $\int_0^\infty d^2\delta/dx^2 dx = 0$, which leads to $C = 0$. We further note that as

$$x \to 0, \quad \frac{d\delta}{dx} = F(-1)\sqrt{x}$$

the above inversion implies that

$$F(-1) = -\frac{2R}{\pi}\int_0^\infty \frac{1}{\sqrt{s}}\frac{d\sigma}{ds}ds$$

The piecewise-linear cohesive zone law has the property that $d\sigma/ds = -d\delta/ds$ on $0 < s < 1$ and 0 for $s > 1$ such that the expression for $F(-1)$ is further reduced to an integral over only the cohesive zone domain,

$$F(-1) = \frac{2R}{\pi}\int_0^1 \frac{1}{\sqrt{s}}\frac{d\delta}{ds}ds = \frac{2R}{\pi}\int_{-1}^0 \frac{F(z)}{1-z}dz = \frac{2R}{\pi}\int_{-1}^0 \sqrt{\frac{1+z}{1-z}}\frac{F(z)}{\sqrt{1-z^2}}dz \approx 1.4262...$$

where the final approximation was calculated using the numerical solution for R and

$$\int_{-1}^0 \sqrt{\frac{1+z}{1-z}}\frac{F(z)}{\sqrt{1-z^2}} \approx \sum_{i=1}^n M_i \sum_{j=1}^n S_{ij}\frac{F(u_j)}{\sqrt{1-u_j^2}} \tag{18}$$

where M_i and S_{ij} are as previously defined in this subsection, and $F(u_j)$ also result from the numerical solution.

4 Non-classical fracture problems and amended asymptotics

In this section we consider an amendment to determine solution procedures for non-classical fracture problems. We define a non-classical problem as one in which fields, such as δ or $d\delta/dx$ near or far behind the tip, or the stress field σ ahead of the tip, follow a power-law in space with an exponent other than one of the classically characteristic values $\pm 1/2$. This simple definition of a non-classical problem includes the problem of a singular crack within a power-law hardening material [e.g., *Hutchinson, 1968*; *Rice and Rosengren, 1968*] as well those involving cracks along a bimaterial interface [e.g., *Rice and Sih*, 1965; *Erdogan, 1965*; *England*, 1965]; however, we limit ourselves into the presumption that the material surrounding the crack responds in a homogenous linearly elastic fashion. Here the non-classical asymptotic behavior arises from the coupling of that elastic response with additional relations to be satisfied along the crack path that are beyond the simple relative-displacement dependent cohesive zone laws examined in the preceding section. The non-classical behavior may arise as a consequence of any number of physical couplings, for examples: the fluid-driven propagation of an open-mode fracture [e.g., *Spence and Sharp*, 1985; *Desroches et al.*, 1994; *Garagash et al.*, 2011]; a rate- and state-dependent friction acting along a sliding interface [*Perrin et al.*, 1995]; frictional heating of the interface of fluid-saturated materials [*Viesca and Garagash*, 2015].

We recall that, to numerically evaluate the finite Hilbert transform of a function $f(s)$, we are interested in finding a decomposition of that function in the form $f(s) = w(s)F(s)$ where $w(s)$ is a known weight function chosen such that $F(s)$ takes on finite values at the endpoints (and, often, is a function to be solved for). When $w(s)$ takes on one of the forms in Table 1, with square-root or inverse square-root asymptotic behavior at the endpoints $s = \pm 1$, the appropriate quadrature to compute the Hilbert transform is known. However, such a decomposition may not be possible when the function $f(s)$ has power-law asymptotics not of the square-root variety. In such cases, we instead look for a decomposition of the form

$$f(s) = w(s)[\Delta F(s) + F^{asy}(s)] \tag{19}$$

where $w(s)$ is restricted to the forms in Table 1, $F^{asy}(s)$ contains the anticipated departure from the square-root asymptotics. This is done as a convenient alternative to directly incorporating the

non-classical asymptotics in the weight function w, in the form $w(s) = (1-s)^\alpha(1+s)^\beta$ where $-1 < \alpha, \beta < 1$. The general set of orthogonal polynomials with such a weight function are the Jacobi polynomials, of which the four kinds of Chebyshev polynomials are the particular sets when α, $\beta = \pm 1/2$. Solutions routes may proceed using expansions in these orthogonal polynomials [e.g., *Erdogan et al.*, 1973] or by integral quadrature, for which *Krenk* [1975a] found general expressions of the appropriate quadrature points and weights for the Cauchy singular integral for the permissible range of exponents α, β. Such routes have been taken for specific problems [e.g., *Adachi and Detournay*, 2002; *Ma and Korsunsky*, 2004]. However, that the well-studied and concisely expressed Chebyshev polynomials permit the ready determination of the quadrature points and weights and methods for interpolation, differentiation, and integration, encourages the search for an amendment, such as that of (19), that permits their continued use. We highlight the practical implementation of such an amendment in two examples to follow: the sliding rupture of a fault aided by thermal pressurization, and the propagation of a hydraulic fracture. These examples also drawn on the other discretization schemes outlined in section 2.

5 Fault rupture facilitated by thermal pressurization

5.1 Problem overview and formulation

We consider the problem of a shear rupture (mode-II or mode-III) of a planar frictional interface within a fluid saturated medium. The shear strength of the interface is assumed to be the product of a constant friction coefficient f and the local effective normal stress on the interface, which is understood to be the difference between the total normal stress (positive in compression) and a pore fluid pressure at the interface. The initial, pre-rupture value of this effective normal stress is denoted as σ_n.

For rupture of a planar interface of elastically identical materials, the total normal stress remains constant at its initial value; however, heating due to frictional sliding can elevate the pore fluid pressure along the ruptured portion of the interface, due to the thermal expansivity of pore water and the porous matrix and the limited flux of pore fluid and heat away from the interface. This weakening process, known as thermal pressurization, and has been a proposed mechanism for strong weakening of interfaces, particularly during the rapid, seismogenic rupture of geologic faults [*Lachenbruch*, 1980; *Mase and Smith*, 1985; *Garagash and Rudnicki*, 2003; *Rice*, 2006]. Three key properties of porous materials in this process are the volumetric heat capacity ρc; a thermal pressurization coefficient Λ (providing the expected increment in pore fluid pressure for a given increment in temperature under conditions in which no fluid flux is permitted); and α, a lumped hydro-thermal diffusivity, defined in terms of the thermal and hydraulic diffusivities of the porous medium (respectively, α_{th} and α_{hy}) as $\alpha = \left(\sqrt{\alpha_{hy}} + \sqrt{\alpha_{th}}\right)^2$.

In this section we search for the crack-tip solution for a rupture propagating at a constant speed v_r. When thermal pressurization results in a complete strength loss far behind the tip (i.e., by complete reduction of the initial effective normal stress), then necessarily the pre-rupture shear stress $\sigma_o(x) = 0$ (i.e., negligible shear stress is needed to propagate the rupture). Taking x to be the moving coordinate whose origin is coincident with the crack tip and positive behind the rupture front, the shear stress along the interface is

$$\sigma(x) = -\frac{\mu'}{2\pi}\int_0^\infty \frac{d\delta/ds}{x-s}ds$$

where μ' is as before for quasi-static rupture propagation and is modified by a mode and rupture-velocity dependent prefactor accounting for the general case of elastodynamic rupture propagation [e.g., *Weertman*, 1969].

The strength behind the rupture front is determined by a Green's function approach to determine the pore pressure increase owed to a continuous, variable heat source behind the rupture front [*Rice*, 2006; *Garagash*, 2012]. The heat source is simply the product of the shear stress and the slip velocity, which is proportional to the spatial gradient of slip in the moving coordinate frame. The resulting expression for the shear strength behind the rupture tip is

$$\sigma(x) = f\sigma_n - \frac{\Lambda}{\rho c}\sqrt{\frac{v_r}{\alpha}}\int_0^x \frac{\sigma(s)\, d\delta/ds}{\sqrt{4\pi(x-s)}}ds \quad \text{for } x > 0$$

where the numerator of the integrand is the variable source term and the denominator is the Green's function.

With $\sigma/(f\sigma_n) \Rightarrow \sigma$, $\delta/\delta_* \Rightarrow \delta$, and $x/x_* \Rightarrow x$, where $x_* = [\rho c\mu'/(f\sigma_n\Lambda)]^2\alpha/v_r$ and $\delta_* = (2f\sigma_n/\mu')x_*$, the problem nondimensionalizes to the pair of equations involving $\sigma(x)$ and $d\delta/ds$

$$\sigma(x) = \frac{1}{\pi}\int_0^\infty \frac{d\delta/ds}{s-x}ds \tag{20a}$$

$$\sigma(x) = 1 - \int_0^x \frac{\sigma(s)d\delta/ds}{\sqrt{\pi(x-s)}}ds \quad \text{for } x > 0 \tag{20b}$$

The latter expression falls in the class of relations identified by (2) and is one that deviates from the classical forms given in section 3 (i.e., an explicitly prescribed spatial distribution $\sigma(x)$ or an explicit relation between σ and δ). As a result, the problem solution exhibits non-classical asymptotic behavior in the far field [*Viesca and Garagash*, 2015]

$$x \to \infty, \quad \frac{d\delta}{dx} = (\pi x)^{-1/4} - \frac{\Gamma(3/4)}{\Gamma(1/4)}x^{-1/2}, \quad \sigma(x) = (\pi x)^{-1/4} \tag{21}$$

In the following subsection we take this non-classical behavior into account in the numerical solution method.

5.2 Numerical procedure and solution

To provide a numerical solution of the full problem posed above, we begin by again using a coordinate transformation to reduce the problem from one on the semi-infinite interval $x \in (0, \infty)$ to the finite interval $z \in (-1, 1)$ via

$$x(z) = \frac{1+z}{1-z},\ \frac{dx}{dz} = \frac{2}{(1-z)^2}$$

such that

$$\sigma[x(z)] = \frac{1-z}{2}\frac{1}{\pi}\int_{-1}^1 \frac{g(u)}{u-z}du$$

$$\sigma[x(z)] = 1 - \int_{-1}^z \sqrt{\frac{1-z}{1-u}}\frac{\sigma[s(u)]g(u)}{\sqrt{2\pi(z-u)}}du$$

where again

$$g(u) = (1-u)\frac{d\delta[s(u)]}{du}$$

When we last considered crack tip problems in section 3.3, we found that the non-singular stress condition at the crack tip and the uniform stress drop in that problem implied the asymptotic scalings $d\delta/ds \sim \sqrt{s}$ as $s \to 0$ and $d\delta/ds \sim 1/\sqrt{s}$ as $s \to \infty$. When accounting for the change of variables, these scalings suggested a decomposition of the form

$$g(u) = \sqrt{\frac{1+u}{1-u}}F(u) \tag{22}$$

However, the far-field asymptotics (21) is not one of a uniform strength drop, but of a gradual decay in strength. Specifically, the near tip field remains $d\delta/ds \sim \sqrt{s}$ as $s \to 0$, but the far-field asymptotic behavior is $d\delta/ds \to As^\gamma$ as $s \to \infty$ where the exponent $\gamma = -1/4$ and the constant $A = (4\pi)^{-1/4}$. The asymptotic decay in strength behind the rupture front is $\sigma(x) \to A\cot(\pi\gamma)x^\gamma$. With these asymptotics in mind we may further decompose (22) by writing

$$F(u) = \Delta F(u) + F^{asy}(u)$$

where F_{asy} provides the correct asymptotic behavior for $g(u)$ as $u \to 1$ if

$$F^{asy}(u) = A\left(\frac{2}{1-u}\right)^{1/2+\gamma}$$

and ΔF will be finite and differentiable at its endpoints.

Substituting the decomposed $g(u)$ into the equation for stress, we may decompose

$$\sigma[x(z)] = \Delta\sigma(z) + \sigma^{asy}(z)$$

where

$$\sigma^{asy}(z) = \frac{1-z}{2}\frac{1}{\pi}\int_{-1}^{1}\sqrt{\frac{1+u}{1-u}}\frac{F_{asy}(u)}{u-z}du$$

$$\Delta\sigma(z) = \frac{1-z}{2}\frac{1}{\pi}\int_{-1}^{1}\sqrt{\frac{1+u}{1-u}}\frac{\Delta F(u)}{u-z}du$$

The latter expression may be approximated using the appropriate quadrature for the Hilbert transform, owing to the regular behavior of $\Delta F(u)$ at its end-points,

$$\Delta\sigma(z_i) = \frac{1}{\pi}\sum_{j=1}^{n} w_j \frac{\Delta F(u_j)}{u_j - z_i} \tag{23}$$

where u_j, z_i, and ω_j are those found in Table 1 corresponding to $w(u) = \sqrt{(1+u)/(1-u)}$. The above provides n equations for $2n$ unknowns $\Delta F(u_j)$ and $\Delta\sigma(z_i)$. Given the known function F_{asy}, the expression for σ_{asy} may be determined analytically or otherwise pre-calculated at the set of points z_i.

Likewise, considering the decomposed strength description

$$\Delta\sigma(z)+\sigma^{asy}(z)=1-\int_{-1}^{z}\sqrt{\frac{1+u}{1-u}}\sqrt{\frac{1-z}{1-u}}\frac{[\Delta\sigma(u)+\sigma^{asy}(u)][\Delta F(u)+F^{asy}(u)]}{\sqrt{2\pi(z-u)}}du$$

we may also precalculate at the set of points z_i the term found on the right hand side

$$s^{asy}(z)=-\int_{-1}^{z}\sqrt{\frac{1+u}{1-u}}\sqrt{\frac{1-z}{1-u}}\frac{\sigma^{asy}(u)F^{asy}(u)}{\sqrt{2\pi(z-u)}}du$$

Consequently, we may write the discretized set of equations as

$$\Delta\sigma(z_i)+\sigma^{asy}(z_i)-s^{asy}(z_i)=1-\sum_{j=1}^{n}S_{ij}M_{ij}\frac{1}{\sqrt{2\pi(u_j-z_i)}}\left\{\left[\sum_{k=1}^{n}L_{jk}\sigma(z_k)\right]F(u_j)-\left[\sum_{k=1}^{n}L_{jk}\sigma^{asy}(z_k)\right]F^{asy}(u_j)\right\} \tag{24}$$

where the matrix S_{ij} is determined by the integration scheme of Section 3 for $w(u)=\sqrt{(1+u)/(1-u)}$; $M_{ij}=\sqrt{(1-z_j)/(1-u_j)}$; and, to evaluate the convolution as a quadrature on u, we have used the interpolation matrix L_{jk} defined for the set of points z_i to interpolate values of σ from the set of points z_i to that of u_j: i.e., we can take the quantities $\sigma(u_j)$ and $\sigma^{asy}(u_j)$ to be approximated by the above terms in square brackets. We have reduced the original problem to a system of $2n$ equations, (23) and (24), for $2n$ unknowns $\Delta\sigma(z_i)$ and $\Delta F(u_j)$. Using the shorthand $\sigma_i=\sigma(z_i)$, $\sigma_j=\sigma(u_j)$, $F_j=F(u_j)$, etc., we may further reduce the expressions of (23) and (24) to

$$\Delta\sigma_i=\frac{1-z_i}{2}\frac{1}{\pi}\sum_{j=1}^{n}w_j\frac{\Delta F_j}{u_j-z_i}$$

$$\Delta\sigma_i+\sigma_i^{asy}-s_i^{asy}=1-\sum_{j=1}^{n}S_{ij}M_{ij}\frac{(\Delta\sigma_j+\sigma_j^{asy})(\Delta F_j+F_j^{asy})-\sigma_j^{asy}F_j^{asy}}{\sqrt{2\pi(u_j-z_i)}}$$

The numerical solution for the slip gradient and the stress, as well as their far-field asymptotic behavior, (21), are illustrated in Figure 4.

6 Propagation of a hydraulic fracture with power-law viscous fluid

6.1 Problem overview and formulation

Here we consider the problem of the propagation of an opening rupture (mode I) that is driven by the pressurization and motion of a power-law fluid within the crack aperture. The medium is under an initial stress state corresponding to a uniform compression, $\sigma_o<0$, acting normal to the eventual rupture plane. The fluid itself may or may not penetrate to the leading edge of the rupture. The latter inability of the viscous fracturing fluid flow to catch up with the moving crack tip results in the fracture tip cavity ("lag") of extent λ filled by the fracturing fluid volatiles or the pore fluid and its volatiles leaked-in from the formation.

The interest in such problems range among the fracturing of rock to enhance hydrocarbon production [e.g., *Detournay*, 2016]; the magma-driven propagation of dikes [e.g., *Rubin*, 1995]; as well as the turbulent drainage of supraglacial lakes [e.g., *Tsai and Rice*, 2010]. The implications of a power-law viscous fluid-driven rupture for behavior near the crack tip was considered by *Desroches*

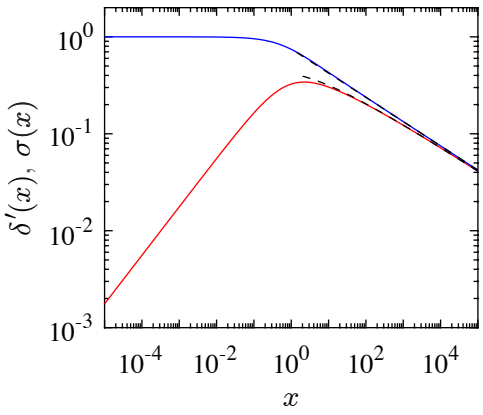

Figure 4: Distributions, as found by numerical solution, of stress (blue) and the gradient of the relative displacement (red) with distance x behind the crack tip of a fracture whose interfacial strength weakens due a frictional-heating induced pressurization of pore fluid. The top black dashed-line is the leading-order asymptotic behavior of both quantities, while the underlying dashed line contains the next-order correction to the asymptotic behavior of the gradient of relative displacement, given in (21).

et al. [1994]; subsequent consideration of fluid lag for a Newtownian (linear) viscous fluid was given by *Garagash and Detournay* [2000]. In this section we formulate the general problem considering both a non-linear viscous fluid and the presence of fluid lag, and outline a procedure for its solutions. We carry out the procedure for the linear viscous case and validate the numerical solutions with the anticipated behavior, while *Moukhtari and Lecampion* [2017] present solutions for non-linear viscous cases.

Again taking x to be the moving coordinate whose origin is coincident with the rupture tip, and positive behind, the normal stress (positive in tension) along the crack path for a rupture propagating at a speed v_r is commonly written for such problems in the form equivalent to (6)

$$\sigma(x) = \sigma_o - \frac{E'}{4\pi}\int_0^\infty \frac{d\delta/ds}{x-s}ds$$

which utlizes the plane-strain modulus $E' = 2\mu'$ where μ' is as previously defined. Moreover, the crack propagation condition requires that $\delta(x) = 4(K/E')\sqrt{2x/\pi}$ where K is the critical mode-I stress intensity factor. We consider that the normal tractions along the crack walls are due to a fluid pressure distribution $p(x)$, i.e.,

$$\sigma(x) = -p(x) \quad \text{for } x > 0$$

and the fluid pressure within the cavity between the rupture and fluid fronts is assumed to have a uniform value p_o, i.e.,

$$p(x) = p_o \quad \text{for } 0 < x < \lambda$$

which can range from near zero (saturated vapor pressure), when compared to the representative stress value σ_o, up to the virgin formation pore pressure value.

Conservation of the incompressible fracturing fluid in the rest of the fracture, together with the Poiseuille law for a power-law fluid ($\tau_f = M\dot{\gamma}^{\mathbf{n}}$ with consistency index M and power-law exponent

$\mathbf{n}$) leads to [e.g. *Desroches et al.*, 1994]

$$v_r^{\mathbf{n}} = \frac{\delta^{\mathbf{n}+1}}{M'}\frac{dp}{dx} \quad \text{for } x > \lambda$$

Here $M' = \psi(\mathbf{n})M$ and $\psi(\mathbf{n}) = 2^{\mathbf{n}+1}(2\mathbf{n}+1)^{\mathbf{n}}/\mathbf{n}^{\mathbf{n}}$.

The above equations govern the solution for the problem in terms of the distribution of the fracture opening $\delta(x)$, the net fluid pressure $p + \sigma_o$, and the extent of the lag λ. We also note that the above formulation for the power-law fluid-driven fracture reduces to that for a Newtonian fluid-driven crack with fully-turbulent Manning-Strickler flow if $\mathbf{n} = 1/3$ and $M' v_r^{\mathbf{n}}$ in the lubrication equation is replaced by $(f_0/4)\rho v_r^2 k^{1/3}$ [see, for example, *Tsai and Rice*, 2010] where $f_0 \approx 0.143$ and k is the fracture wall roughness.

With $(p + \sigma_o')/\sigma_o' \Rightarrow p$, $\delta/\delta_* \Rightarrow \delta$, $x/x_* \Rightarrow x$, $K/(\sigma_o'\sqrt{\pi x_*/2}) \Rightarrow \kappa$, $\lambda/x_* \Rightarrow \lambda$, where x_* is the lengthscale

$$x_* = \frac{(E'/4)^{1+1/\mathbf{n}} M'^{1/\mathbf{n}} v_r}{\sigma_o'^{1+2/\mathbf{n}}} \tag{25}$$

$\delta_* = (4\sigma_o'/E')x_*$, and $\sigma_o' = -(\sigma_o + p_o)$ is the underpressure in the lag, the problem non-dimensionalizes to the following equations involving $p(x)$ and $\delta(x)$

$$p(x) = \frac{1}{\pi}\int_0^\infty \frac{d\delta/ds}{x-s} ds$$

$$p(x) = -1 \quad \text{for } 0 < x \le \lambda$$

$$\delta^{\mathbf{n}+1}\frac{dp}{dx} = 1 \quad \text{for } x > \lambda$$

with the additional constraint that

$$\delta(x) = \kappa\sqrt{x} \quad \text{as } x \to 0 \tag{26}$$

The solution for λ, $p(x)$ and $\delta(x)$ is a function of a single parameter $0 \le \kappa < \infty$. As noted by *Garagash and Detournay* [2000], it is advantageous for numerical solutions to instead parameterize the problem by λ, leaving κ as one of the solution variables. We note that for the Newtonian fluid case ($\mathbf{n} = 1$), the scaling reduces to that of *Garagash and Detournay* [2000] up to the prefactor in the expression for the lengthscale, specifically $x_* = L_\mu/4^2$ in terms of the L_μ used by these authors. The difference stems from the use of $E'/4$ in (25) rather than E' in the work of *Garagash and Detournay* [2000].

As an aside, in the particular case of zero toughness ($\kappa = 0$), the more direct route to the solution is to prescribe a zero toughness value and solve for the lag. In this case, we will resort to solving the problem in a different scaling: $(p + \sigma_o)/\sigma_o' \Rightarrow p$, $\delta/(4\lambda\sigma_o'/E') \Rightarrow \delta$, $x/\lambda \Rightarrow x$, $K/(\sigma_o'\sqrt{\pi\lambda/2}) \Rightarrow \kappa$, $\lambda/x_* \Rightarrow \lambda$. In this scaling, the normalized position of the fluid front in the crack is at $x = 1$, and the lubrication equation is modified to $\delta^{\mathbf{n}+1} dp/dx = \lambda^{-\mathbf{n}}$ (for $x > 1$).

To leading order, the solution to the problem possesses a non-classical behavior of the solution in the far field, $x \to \infty$, corresponding to the far-field behavior of the propagating fracture in the absence of a cavity (i.e., the presence of the fluid lag and finite toughness encountered at the crack

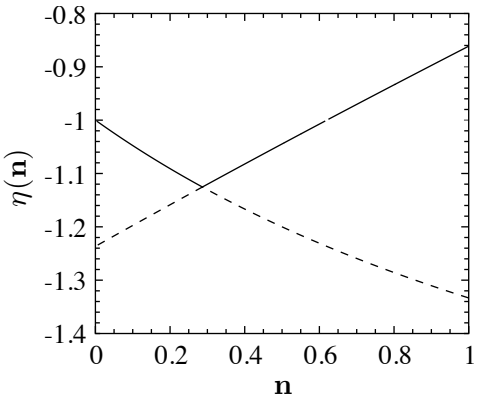

Figure 5: Solution to the transcendental equation (27) for the exponent η of the next-order term of the far-field asymptotics for fluid pressure and the gradient of relative displacement. The solution for η is given as it depends on the exponent $\mathbf{n}$ of the power-law viscous fluid. There are two solution branches and the appropriate value for η is given by the greatest value of the two (solid line), which is well approximated by a bilinear function defined by three points $(\mathbf{n}, \eta) = (0, -1)$, $(-0.2866, -1.1254)$, and $(1, -0.86133)$.

tip is not apparent to the leading order of the solution in the far-field), which is [*Desroches* et al., 1994]

$$x \to \infty, \quad \frac{d\delta}{dx} = Ax^{\gamma}, \quad p(x) = A\cot(\pi\gamma)x^{\gamma}$$

where the exponent $\gamma = -\mathbf{n}/(2+\mathbf{n}) \leq 0$ and assumes a value of 0 for a Bingham fluid ($\mathbf{n} = 0$) and a value of $-1/3$ for a Newtonian fluid ($\mathbf{n} = 1$), while the prefactor $A = (1+\gamma)[\gamma(1+\gamma)\cot(\pi\gamma)]^{-(1+\gamma)/2}$. (The case of the Bingham fluid is obtained in the limit $\gamma \to 0$ of the above asymptotic form, leading to $d\delta/dx = A = \sqrt{\pi}$ and $p(x) = \ln x/\sqrt{\pi} + \text{constant}$.) The next-order correction to the above far-field asymptotic behavior can be obtained, by extending the analysis of *Garagash and Detournay* [2005]

$$x \to \infty, \quad \frac{d\delta}{dx} = Ax^{\gamma} + Bx^{\eta}, \quad p(x) = A\cot(\pi\gamma)x^{\gamma} + B\cot(\pi\eta)x^{\eta}$$

where the exponent $\eta(\mathbf{n})$ is the solution of the transcendental equation

$$\frac{\eta(1+\eta)\cot(\pi\eta)}{\gamma(1-\gamma)\cot(\pi\gamma)} = -1 \tag{27}$$

as shown in Figure 5. The influence of the near-tip processes due to the toughness and the fluid lag are included in the coefficient B (i.e., $B(\lambda)$ or $B(\kappa)$, depending on the problem parameterization), which cannot be determined from the asymptotic analysis alone and, therefore, is part of the full solution.

6.2 Numerical procedure and solution

We begin following the mapping of the semi-infinite crack on $x \in (0, \infty)$ to $z \in (-1, 1)$ by $x = (1+z)/(1-z)$, which transforms the equations governing crack opening and fluid pressure

distribution is the requirement that

$$\delta[x(z)]^{\mathbf{n}+1}\frac{dx}{dz}\frac{dp}{dz}=1 \quad \lambda_z<z<1$$

$$p[x(z)]=-1 \quad 0<z\leq\lambda_z$$

where $\lambda_z=(\lambda-1)/(\lambda+1)$ is the mapped position of the fluid front, as well as

$$\frac{1}{\pi}\int_{-1}^{1}\frac{g(u)}{z-u}=h(z)$$

where

$$g(u)=(1-u)\frac{d\delta}{du} \quad h(z)=2\frac{p[x(z)]}{1-z}$$

with the propagation condition

$$g(u)=\kappa\sqrt{\frac{2}{1+u}}, \quad u\to-1$$

We look for the solution in the form of the decomposition

$$g(u)=\frac{1}{\sqrt{1-u^2}}\left[F(u)+F^{asy}(u)\right]$$

where F^{asy} provides the correct asymptotic behavior of $g(u)$ as $u\to 1$ if

$$F^{asy}(u)=2A\frac{1+u}{2}\left(\frac{2}{1-u}\right)^{1/2+\gamma}$$

while also ensuring that there is no contribution of F^{asy} to the crack-tip singularity (i.e., $F^{asy}(-1)=0$). Thus, the regular part $\Delta F(u)$ is continuous and differentiable at the interval's ends, and is constrained by the propagation condition as $\Delta F(-1)=\kappa$. We may decompose the net fluid pressure and crack opening as

$$p[x(z)]=\Delta p(z)+p^{asy}(z)$$

$$\delta[x(z)]=\Delta\delta(z)+\delta^{asy}(z)$$

where we denote the contributions of F^{asy} to each as

$$p^{asy}(z)=\frac{(1-z)}{2}\frac{1}{\pi}\int_{-1}^{1}\frac{1}{\sqrt{1-u^2}}\frac{F^{asy}(u)}{z-u}du$$

$$\delta^{asy}(z)=\int_{-1}^{z}\frac{1}{\sqrt{1-u^2}}\frac{F^{asy}(u)}{1-u}du$$

Using the Gauss-Chebyshev discretization with the weight function $w(z)=1/\sqrt{1-z^2}$ to discretize $\Delta F_j=\Delta F(u_j)$, $p_i=p[x(z_i)]$, $\delta_i=\delta[x(z_i)]$, etc., (where the points u_j and z_i, and weights w_j to follow are those found in Table 1) we can write the discretized set of governing equations as

$$\Delta p_i=\frac{1-z_i}{2}\frac{1}{\pi}\sum_{j=1}^{n}w_j\frac{\Delta F_j}{z_i-u_j}$$

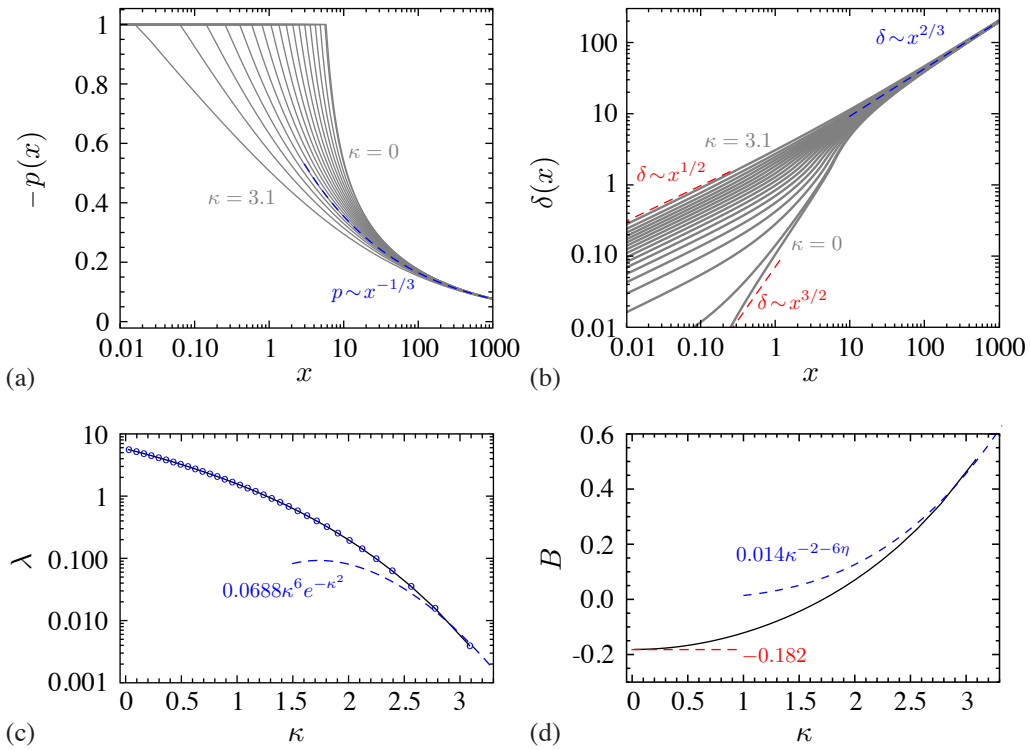

Figure 6: Distributions of (a) stress and (b) relative displacement with distance behind the rupture front for a rupture driven by a Newtonian viscous fluid with variable values of fracture toughness κ, with universal far-field asymptotic behavior (blue-dashed). Red-dashed lines in (b) show transition in near-tip asymptotic behavior as fracture toughness vanishes. (c) A fluid lag λ exists and depends on the fracture toughness κ, with the large toughness asymptotic behavior of *Garagash and Detournay* [2000] shown as a blue dashed line. (d) The coefficient B of the next-order correction to the far-field asymptotics for stress and displacement, as it depends on the fracture toughness. The large-toughness asymptotic behavior is shown as a dashed blue line [*Garagash and Detournay*, 2005]. Solutions shown are for $n = 200$.

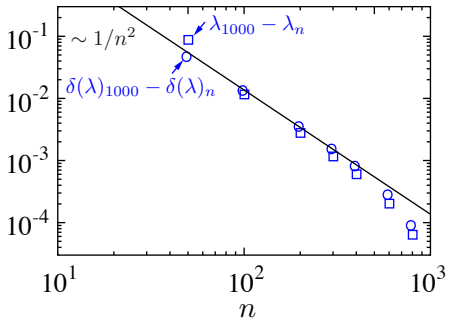

Figure 7: Convergence of the zero-toughness Newtonian hydraulic fracture tip solution with respect to the reference numerical solution, in which $n = 1000$. The straight line indicates a $\sim 1/n^2$ slope.

with

$$p_i = -1, \quad p_i = p_i^{asy} + \Delta p_i \quad -1 < z_i \le z_{i_\lambda} \tag{28a}$$

$$\delta_i^{\mathbf{n}+1} \left(\frac{dz}{dx}\right)_i \left(\frac{dp}{dz}\right)_i = 1, \quad \left(\frac{dp}{dz}\right)_i = \left(\frac{dp^{asy}}{dz}\right)_i + \sum_{i'=1}^{n-1} D_{ii'} \Delta p_{i'} \quad z_i > z_{i_\lambda} \tag{28b}$$

where grid point $z_{i_\lambda} = \lambda_z$ corresponds to the prescribed location of the fluid front; $(dz/dx)_i = (1 - z_i^2)/2$; and the differentiation matrix $D_{ii'}$ on the set of points z_i is determined analogously to $D_{jj'}$ in (5) by using appropriate weights ω_i in Table 3. The crack opening is given by

$$\delta_i = \delta_i^{asy} + \sum_{j=1}^{n} S_{ij} \frac{\Delta F_j}{1 - u_j}$$

where S_{ij} is determined by the integration scheme of Section 3 for $w(u) = \sqrt{(1+u)/(1-u)}$. The values of δ_i^{asy}, p_i^{asy}, and $(dp^{asy}/dz)_i$ may be precalculated. The system of $2(n-1)$ equations is complemented by the propagation condition and by the condition of the vanishing net pressure at the far field

$$\sum_{j=1}^{n} P_j \Delta F_j = \Delta F(-1) = \kappa$$

$$\sum_{i=1}^{n-1} Q_i \Delta p_i = \Delta p(1) = 0$$

to yield an algebraic system of $2n$ equations for $2n$ unknowns ΔF_j, Δp_i, and κ.

As a final note on the numerical method of the solution, we acknowledge that the fluid pressure gradient in the crack is discontinuous at the fluid front, which is expected to severely limit the accuracy of Gauss-Chebyshev differentiation (otherwise spectral for regular, infinitely differentiable functions) in the discretized lubrication equation (28b). In order to improve the accuracy of the

discrete differentiation of a function $\Delta p[x(z)]$ with a discontinuous derivative at $z = z_{i_\lambda}$, we replace it with its "to-the-left" continuation

$$\Delta p_{\leftarrow}[x(z)] \equiv \Delta p[x(z)] + J_\lambda (z - z_{i_\lambda}) H(z_{i_\lambda} - z)$$

where $H(z)$ is the Heaviside unit-step function, and

$$J_\lambda = \left(\frac{dp}{dz}\right)_{z_{i_\lambda}+0} - \left(\frac{dp}{dz}\right)_{z_{i_\lambda}-0} \approx \frac{p_{i_\lambda-1} - p_{i_\lambda}}{z_{i_\lambda-1} - z_{i_\lambda}} - \frac{p_{i_\lambda+1} - p_{i_\lambda}}{z_{i_\lambda+1} - z_{i_\lambda}}$$

is the derivative jump approximated by a finite difference. We observe that the function $\Delta p_{\leftarrow}[x(z)]$ is everywhere differentiable with its values given by the original function $\Delta p[x(z)]$ in $z > z_{i_\lambda}$ and by that superimposed with a linear function $J_\lambda(z - z_{i_\lambda})$ in $z < z_{i_\lambda}$.

The general problem solutions ($\kappa \geq 0$) are presented in Figure 6. The convergence of the method is evaluated for the zero-toughness ($\kappa = 0$) case and presented in Figure 7.

7 Summary and Conclusion

We consider numerical solutions to linear elastic fracture problems in which crack-face tractions and relative displacement are coupled both by the elasticity of the continuum containing the crack as well as by any number of additional physical processes. We begin by highlighting that the quadrature of *Erdogan et al.* [1973] for the numerical evaluation of the characteristic singular integral for crack problems, with collocation points occurring at the nodes of Chebyshev polynomials, allows for the ready evaluation with potential for spectral accuracy of other operations that may arise in constraints on relations among crack-face tractions, relative displacement, or other field variables provided by the additional processes. We provide the necessary coefficients and weights to integrate, differentiate, and interpolate functions whose values are known at a set of points lying at the nodes of one of the four kinds of Chebyshev polynomials.

We highlight the convenience and accuracy of this approach by first considering classical problems in fracture mechanics, focusing on finite or semi-infinite cracks that are singular or obey cohesive-zone traction-separation relations. Such problems have classical square-root asymptotics appropriate for the singular integral quadrature and may have a single solution or a one-parameter family of solutions and we detail procedures to find numerical solutions to such problems using the aforementioned numerical methods. Among the results, we show that the smoothness of the cohesive-zone relation imposes limits on the order of convergence of numerical solutions and we provide conditions in which spectral accuracy may be achieved.

We finally consider the convenience the method provides for the numerical solution of fracture problems with non-classical asymptotic behavior, owed to specific physical processes. The first problem considered is the propagation of a sliding-mode rupture facilitated by the pressurization of pore fluid at the interface due to rapid frictional shear heating. The second problem is the propagation of an open-mode hydraulic fracture in a material of finite or negligible fracture toughness driven by a power-law fluid. In addition to the evaluation of the singular integral, the solution to these problems requires differentiation, integration, and interpolation. Furthermore, while each problem lacks classical square-root asymptotics we show that we may continue to make convenient use of the numerical methods with a slight amendment in the solution procedure.

A Results on smoothness of function and its Hilbert transform

A.1 A discontinuity in stress or one of its derivatives within an interior point

We begin by considering the equation relating stress with the gradient of relative displacement for an in-plane or anti-plane of finite extent

$$\sigma(x) = \sigma_o(x) - \frac{1}{\pi}\int_{-1}^{1} \frac{d\delta/ds}{x-s} ds \tag{A.1}$$

We further presume that a discontinuity in $\sigma(x)$ exists at $x = b$ for some $|b| < 1$: i.e., $\sigma(b^+) - \sigma(b^-) = \Delta\sigma$. To examine behavior in the vicinity of the discontinuity, we use the following coordinate transformation to center on and expand about the discontinuity: $(x-b)/\epsilon \Rightarrow x$ with $\delta/\epsilon \Rightarrow \delta$, where we take the limit that $\epsilon \to 0$. In this limit, the discontinuity $\sigma(x)$ appears, to within a constant, as a Heaviside step function of height $\Delta\sigma$. Furthermore, if $\sigma_o(x)$ is continuous at b, $\sigma_o(x)$ appears to take on a constant value: i.e., $\sigma_o(x) \to \sigma_o(b) = \sigma_b$. Thus, following the transformation, (A.1) reduces to

$$\sigma(x) = \sigma_b - \frac{1}{\pi}\int_{-\infty}^{\infty} \frac{d\delta/ds}{x-s} ds \tag{A.2}$$

which inverts to

$$\frac{d\delta}{dx} = \frac{1}{\pi}\int_{-\infty}^{\infty} \frac{\sigma(s) - \sigma_b}{x-s} ds \tag{A.3}$$

Following an integration by parts,

$$\frac{d\delta}{dx} = -\frac{1}{\pi}\left[\sigma(s)\ln|x-s|\right]_{-\infty}^{\infty} + \frac{1}{\pi}\int_{-\infty}^{\infty} \frac{d\sigma(s)}{ds}\ln|x-s|\, ds \tag{A.4}$$

Given that $\sigma(x)$ appears a step function, $d\sigma/dx = \Delta\sigma\delta_D(x)$, where $\delta_D(x)$ denotes the Dirac delta. Substituting this expression in (A.4), we find that the discontinuity in $\sigma(x)$ at $x = 0$ leads to a logarithmic singularity there for $d\delta/dx$, i.e.,

$$|x| \to 0, \quad \frac{d\delta}{dx} = \frac{\Delta\sigma}{\pi}\ln|x| \tag{A.5}$$

We may similarly show that a discontinuity in the m-th derivative of $\sigma(x)$ leads to a logarithmic singularity in the m-th derivative of $d\delta/dx$. This is done by first noting that the convolution on the right hand side of (A.2) is the Hilbert transform $\mathcal{H}(d\delta/dx)$, for which $d\mathcal{H}[f(x)]/dx = \mathcal{H}(df/dx)$ [e.g., *King*, 2009]. Following m spatial derivatives of (A.2), we may arrive at the desired result by following the steps reflected in (A.3–A.5). Such discontinuities in σ may arise, for example, from discontinuities first encountered in the m-th derivative with respect to δ of a cohesive zone law $\sigma[\delta(x)]$

$$\frac{d^m\sigma}{dx^m} = \frac{d^m\sigma}{d\delta^m}\left(\frac{d\delta}{dx}\right)^m + \frac{d\sigma}{d\delta}\frac{d^m\delta}{dx^m} + \ldots$$

where the remainder consists of terms whose highest derivative is of order less than m. The discontinuity in $d^m\sigma/d\delta^m$ is thus reflected as a logarithmic singularity in $d^{m+1}\delta/dx^{m+1}$ with all lower-ordered derivatives of $\delta(x)$ being continuous at the point of the discontinuity.

A.2 Cohesive-zone relations and singularities at the crack tip

We consider a cohesive zone relation in the form $\sigma(\delta)$ such that we may write

$$\sigma[\delta(x)] = \sigma_o(x) - \frac{1}{\pi}\int_{-1}^{1} \frac{d\delta/ds}{x-s} ds \tag{A.6}$$

We recall that the quadrature of the integral transform for such a problem calls for a decomposition in the form of $d\delta/dx = \sqrt{1-x^2}F(x)$. Here we will show that any $\sigma(\delta)$ with a Taylor expansion about $\delta = 0$ containing odd powers will lead to a logarithmic singularity in a derivative of $F(x)$ at the crack tips $x = \pm 1$.

To examine the asymptotic behavior approaching the crack tip, say, at $x = -1$, we use the following coordinate transformation: $(x+1)/\epsilon \Rightarrow x$, such that the tip now corresponds to $x = 0$, $\delta/\epsilon \Rightarrow \delta$, and $\sqrt{\epsilon}F \Rightarrow F$. Similarly to the transformation in the previous subsection, we consider the limit $\epsilon \to 0$. In this limit $\sigma_o(x) \to \sigma_o(0) = \sigma_0$, such that (A.6), following the transformation, reduces to

$$\sigma(x) = \sigma_0 - \frac{1}{\pi}\int_{0}^{\infty} \frac{d\delta/ds}{x-s} ds \tag{A.7}$$

which inverts to

$$\frac{d\delta}{dx} = \frac{\sqrt{x}}{\pi}\int_{0}^{\infty} \frac{1}{\sqrt{s}} \frac{\sigma(s)-\sigma_o}{x-s} ds \tag{A.8}$$

We now consider that the cohesive zone law $\sigma[\delta(x)]$ has a Taylor expansion about $\delta = 0$ in the form

$$\sigma(x) = \sigma(0) + A\delta(x) + B\delta(x)^2 + ... \tag{A.9}$$

Since, for a non-singular crack, $\delta(x) = Cx^{3/2}$ to leading order in x, the leading contribution from each term in the expansion of the cohesive zone law in δ results in

$$\frac{d\delta}{dx} = \frac{\sqrt{x}}{\pi}\int_{0}^{\infty} \frac{1}{\sqrt{s}} \frac{\sigma(0)-\sigma_0 + \hat{A}s^{3/2} + \hat{B}s^3 ...}{x-s} ds \tag{A.10}$$

where $\hat{A} = AC$, and $\hat{B} = BC^2$. Evaluating (A.10) with a finite upper limit x_o leads to

$$\frac{d\delta}{dx} = (\sigma(0)-\sigma_o)(a_1 x^{1/2} + a_2 x^{3/2} + a_3 x^{5/2} + ...) \tag{A.11}$$

$$+ \hat{A}(b_1 x^{1/2} + b_2 x^{3/2}\ln(x/x_o) + b_3 x^{5/2} + ...) \tag{A.12}$$

$$+ \hat{B}(c_1 x^{1/2} + c_2 x^{3/2} + c_3 x^{5/2} + ...) + ... \tag{A.13}$$

where a_n, b_n, and c_n are constants.

Since, following our coordinate transformation, $d\delta/dx = \sqrt{2x}F(x)$ as $x \to 0$ we can conclude that the linear term in the cohesive zone law expansion near the crack tip (A.9), when non-zero, leads to a logarithmic singularity at the crack tip in $F'(x)$. We can likewise show that the presence of any odd term in the expansion (A.9) (e.g., linear, cubic, etc.), leads to a logarithmic singularity at the crack tip in the $(3m-1)/2$-th derivative of $F(x)$, where m is the exponent of the leading order odd term in the expansion: e.g., if a cubic (and no linear) term is present in (A.9), then $m = 3$ and a logarithmic singularity appears in $F^{(4)}(x)$ at $x = \pm 1$. This establishes that $F(x)$ is

a regular (infinitely differentiable) function at the crack tip when and only when $d^m\sigma/\delta^m = 0$ at $\delta = 0$ for all odd m. An example of such a cohesive law, $\sigma(\delta) = \exp(-\delta^2)$, was explored in the main text.

Acknowledgements

RCV is grateful for support from NSF grants EAR-1344993 and EAR-1653382. DIG acknowledges the support from the Natural Science and Engineering Research Council of Canada under Discovery grant 05743 and Collaborative Research and Development grant CRDPJ 452752.

References

Adachi, J. I., and E. Detournay (2002), Self-similar solution of a plane-strain fracture driven by a power-law fluid, *Int. J. Numer. Anal. Met.*, *26*, 579–604.

Berrut, J.-P., and L. N. Trefethen (2004), Barycentric Lagrange interpolation, *SIAM Rev.*, *46*(3), 501–517.

Boyd, J. P. (2001), *Chebyshev and Fourier Spectral Methods*, Dover, New York.

Brantut, N., and R. C. Viesca (2015), Earthquake nucleation in intact or healed rocks, *J. Geophys. Res. Solid Earth*, *120*(1), 191–209.

Dempsey, J. P., L. Tan, and S. Wang (2010), An isolated cohesive crack in tension, *Continuum Mech. Thermodyn.*, *22*(6-8), 617–634.

Desroches, J., E. Detournay, B. Lenoach, P. Papanastasiou, J. R. A. Pearson, M. Thiercelin, and A. Cheng (1994), The crack tip region in hydraulic fracturing, *P. Roy. Soc. A.*, *447*(1929), 39–48.

Detournay, E. (2016), Mechanics of hydraulic fractures, *Annu. Rev. Fluid Mech.*, *48*(1), 311–339.

Erdogan, F., G. D. Gupta, and T. S. Cook (1973), Numerical solution of singular integral equations, in *Methods of Analysis and Solutions of Crack Problems, Mechanics of Fracture Series*, edited by G. C. Sih, pp. 368–425, Noordhoff Int. Pub.

Garagash, D., and E. Detournay (2000), The tip region of a fluid-driven fracture in an elastic medium, *J. Appl. Mech.*, *67*(1), 183–192.

Garagash, D. I. (2012), Seismic and aseismic slip pulses driven by thermal pressurization of pore fluid, *J. Geophys. Res.*, *117*(B4), B04,314.

Garagash, D. I., and E. Detournay (2005), Plane-strain propagation of a fluid-driven fracture: small toughness solution, *J. Appl. Mech.*, *72*(6), 916–928.

Garagash, D. I., and J. W. Rudnicki (2003), Shear heating of a fluid-saturated slip-weakening dilatant fault zone 1. Limiting regimes, *J. Geophys. Res.*, *108*(B2), 2121.

Garagash, D. I., E. Detournay, and J. I. Adachi (2011), Multiscale tip asymptotics in hydraulic fracture with leak-off, *J. Fluid Mech.*, *669*, 260–297.

Hills, D. A., P. A. Kelley, D. N. Dai, and A. M. Korsunsky (1996), *Solution of Crack Problems*, Kluwer Academic Publishers, Dordrecht.

Hutchinson, J. W. (1968), Singular behaviour at the end of a tensile crack in a hardening material, *J. Mech Phys. Solids*, *16*(1), 33–31.

Ida, Y. (1972), Cohesive force across tip of a longitudinal-shear crack and griffiths specific surface-energy, *J. Geophys. Res.*, *77*(20), 3796–3805.

Krenk, S. (1975a), On quadrature formulas for singular integral equations of the first and the second kind, *Q. Appl. Math.*, *33*(3), 225–232.

Krenk, S. (1975b), Use of Interpolation Polynomial for Solutions of Singular Integral-Equations, *Q. Appl. Math.*, *32*(4), 479–484.

Lachenbruch, A. H. (1980), Frictional heating, fluid pressure, and the resistance to fault motion, *J. Geophys. Res.*, *85*, 6097–6112.

Ma, L., and A. M. Korsunsky (2004), A note on the Gauss-Jacobi quadrature formulae for singular integral equations of the second kind, *Int. J. Fract.*, *126*, 399–405.

Mase, C. W., and L. Smith (1985), Pore-fluid pressures and frictional heating on a fault surface, *Pure. Appl. Geophys.*, *122*(2-4), 583–607.

Mason, J. C., and D. C. Handscomb (2003), *Chebyshev Polynomials*, Chapman & Hall, London.

Moukhtari, F.-E., and B. Lecampion (2017), A semi-infinite hydraulic fracture driven by a shear thinning fluid, *J. Fluid Mech.*, *submitted*.

Palmer, A. C., and J. R. Rice (1973), Growth of slip surfaces in progressive failure of over-consolidated clay, *P. Roy. Soc. Lond. A*, *332*(1591), 527–548.

Perrin, G., J. R. Rice, and G. Zheng (1995), Self-healing slip pulse on a frictional surface, *J. Mech Phys. Solids*, *43*(9), 1461–1495.

Powell, M. J. D. (1981), *Approximation Theory and Methods*, Cambridge University Press, Cambridge.

Rice, J. R. (1968), Mathematical analysis in the mechanics of fracture, in *Fracture, An Advanced Treatise*, edited by H. Liebowitz, pp. 191–311, Academic Press, New York.

Rice, J. R. (2006), Heating and weakening of faults during earthquake slip, *J. Geophys. Res.*, *111, B05311*.

Rice, J. R., and G. F. Rosengren (1968), Plane strain deformation near a crack tip in a power-law hardening material, *J. Mech Phys. Solids*, *16*(1), 1–12.

Rice, J. R., and G. C. Sih (1965), Plane problems of cracks in dissimilar media, *J. Appl. Mech.*, *32*(2), 418–423.

Rubin, A. M. (1995), Propagation of magma-filled cracks, *Annu. Rev. Earth Pl. Sc.*, *23*(1), 287–336.

Spence, D. A., and P. Sharp (1985), Self-similar solutions for elastohydrodynamic cavity flow, *Proc. Roy. Soc. Lond. A*, *400*(1819), 289–313.

Tsai, V. C., and J. R. Rice (2010), A model for turbulent hydraulic fracture and application to crack propagation at glacier beds, *J. Geophys. Res.*, *115, F03007*.

Viesca, R. C., and D. I. Garagash (2015), Ubiquitous weakening of faults due to thermal pressurization, *Nature Geoscience*, *8*(11), 875–879.

Viesca, R. C., and J. R. Rice (2012), Nucleation of slip-weakening rupture instability in landslides by localized increase of pore pressure, *J. Geophys. Res.*, *117*(B3), B03,104.